NASA Contractor Report 172171

ICASE

RADIATION OF SOUND FROM UNFLANGED CYLINDRICAL DUCTS

S. I. Hariharan

and

A. Bayliss

Contract No. NAS1-17070
July 1983

INSTITUTE FOR COMPUTER APPLICATIONS IN SCIENCE AND ENGINEERING
NASA Langley Research Center, Hampton, Virginia 23665

Operated by the Universities Space Research Association

RADIATION OF SOUND FROM UNFLANGED CYLINDRICAL DUCTS

S. I. Hariharan
Institute for Computer Applications in Science and Engineering
NASA Langley Research Center, Hampton, VA 23665

Alvin Bayliss
Exxon Corporate Research
Linden, NJ 07036

ABSTRACT

In this paper we present calculations of sound radiated from unflanged cylindrical ducts. The numerical simulation models the problem of an aero-engine inlet. The time-dependent linearized Euler equations are solved from a state of rest until a time harmonic solution is attained. A fourth-order accurate finite difference scheme is used. Solutions are obtained from a fully vectorized Cyber-203 computer program. Cases of both plane waves and spin modes are treated. Spin modes model the sound generated by a turbofan engine. Boundary conditions for both plane waves and spin modes are treated. Solutions obtained are compared with experiments conducted at NASA Langley Research Center.

Research was supported by the National Aeronautics and Space Administration under NASA Contract No. NAS1-17070 while the authors were in residence at ICASE, NASA Langley Research Center, Hampton, VA 23665. Work for the second author was also supported by the U. S. Department of Energy, Contract No. TE/AC02/76ER03077 and by the Air Force Contract No. AFOSR/81/0020.

INTRODUCTION

In this paper we present a computational method to study sound radiated from an unflanged cylindrical duct. An incident field which is either a plane wave or a spinning mode (i.e., dependence on the azimuthal angle) propagates down the duct. At the open end of the duct, sound is radiated out into the farfield and a reflected wave traveling upstream in the duct is generated. This problem is of importance in the study of noise radiated from aero-engine inlets and in the development of effective duct liners.

A significant amount of work has been done on the computation of sound propagation in an infinitely long duct. A survey of such work may be found in [1]. The open end of the duct and the ensuing outward radiation of energy significantly complicates the problem. A further complication is the presence of the inlet flow about which little is known experimentally. In the procedure adapted here the solution is obtained by solving the Euler equations linearized about an arbitrary mean flow. Thus the method is general enough to permit computation of the linearized fluctuating field about an experimentally determined mean flow. However, in this paper only the case of no mean flow is considered.

We will briefly discuss some work which has been done in the past and is relevant to our work. The earliest work in calculating the sound wave (pressure) radiated from cylindrical ducts is due to Levine and Schwinger [8]. They provided a method to predict sound from a semi-infinite thin pipe, when a plane wave is incident upstream in the pipe, using the Weiner-Hopf technique. This work motivated several other researchers in this field, in particular Savkar [10] provided a method to predict sound using Weiner-Hopf techniques for the case of an incident spinning mode. Ting and Keller [13] developed an asymptotic expansion valid for plane wave incidence and flow frequencies. For

higher frequencies asymptotic methods have not been successfully applied to this problem because there are different length scales inside the pipe and in the farfield. Though these methods provide some means to compute the sound radiated from engine inlets, they do not correspond to the entire physical situation due to the thickness of the inlets. With a given thickness of the duct and for smooth geometries, calculations are effectively handled by integral equation methods. One such work is due to Horowitz, et al. [5]. This method is based on a Helmholtz equation approach for the fluctuating sound pressure field and does not have the means to incorporate a mean flow. Thus a method is needed to study the radiation of sound that has the capability of handling flows. This is the motivation of this paper.

2. FORMULATION OF THE PROBLEM

We obtain the field equations from the fluid equations. The equations of inviscid flow with the standard summation convention can be written as a first order system

$$\begin{aligned} &\frac{\partial \rho}{\partial t} + \operatorname{div}(\rho \underline{v}) = 0 \\ &\rho\left(\frac{\partial v_i}{\partial t} + v_j \frac{\partial v_i}{\partial x_j}\right) + \frac{\partial p}{\partial x_i} = 0. \end{aligned} \tag{2.1}$$

Here ρ is the density, v the velocity, and p is the pressure. We divide the flow variables into mean and fluctuating parts. We thus write

$$\begin{aligned} \rho &= \overline{\rho} + \rho' \\ \underline{v} &= \underline{\overline{U}} + \underline{u}' \\ p &= \overline{p} + p' , \end{aligned} \tag{2.2}$$

where the bar denotes a mean quantity independent of time. We reformulate the resulting system by replacing the fluctuating density ρ' by the fluctuating pressure p' which is the common acoustic variable. We assume that the flow is homentropic and has no mean temperature gradient. It then follows that

$$p = A\,\rho^{\gamma} \tag{2.3}$$

or

$$\rho' = \frac{p'}{c_0^2} + O(p'^2), \tag{2.4}$$

where c_0 is the ambient speed of sound. Thus the resulting system from (2.1) becomes

$$\begin{aligned} &\frac{1}{c_0^2}\frac{\partial p'}{\partial t} + \frac{1}{c_0^2}\,\mathrm{div}(p'\underline{\bar{U}}) + \mathrm{div}(\bar{\rho}\underline{u}') = -\mathrm{div}(\bar{\rho}\,\underline{\bar{U}}) + q \\ &\bar{\rho}\Big(\frac{\partial u_i'}{\partial t} + U_j\frac{\partial u_j'}{\partial x_j} + u_j'\frac{\partial \bar{U}_i}{\partial x_j}\Big) + \frac{p'}{c_0^2}\bar{U}_j\frac{\partial \bar{U}_i}{\partial x_j} + \frac{\partial p'}{\partial x_i} = -\frac{\partial \bar{p}}{\partial x_i} - \bar{\rho}\,\bar{U}_j\frac{\partial \bar{U}_i}{\partial x_j} + q, \end{aligned} \tag{2.5}$$

where q denotes higher-order terms containing p'^2, $p'u'$, u'^2, etc. The left hand of system (2.5) contain the first order interacting terms between the fluctuating and mean quantities. The right hand side contain the mean flow and fluctuating quantities of the lower order terms. In general the system (2.5) is a linear first-order hyperbolic system which includes all of the first-order terms for the fluctuating field subject to a time-dependent inflow condition.

For the present purpose we assume the mean flow is zero. Thus the system (2.5) reduces to

$$\frac{1}{c_0^2}\frac{\partial p'}{\partial t} + \rho_0 \operatorname{div} \underline{u}' = 0$$

$$\rho_0 \frac{\partial \underline{u}'}{\partial t} + \nabla p' = 0, \tag{2.6}$$

where ρ_0 is the density of the ambient fluid. We non-dimensionalize these equations. Length is non-dimensionalized by the diameter of the pipe (d), time by c_0/d, pressure by $\rho_0 c_0^2$ and the velocity by c_0 to obtain

$$\frac{\partial p}{\partial t} + \operatorname{div} \underline{u} = 0$$

$$\frac{\partial \underline{u}}{\partial t} + \nabla p = 0. \tag{2.7}$$

Note that in (2.7) the prime on the fluctuating quantities are dropped for convenience.

REMARK 2.1: If p and u are time harmonic, that is

$$p(x,t) = \hat{p}(x)e^{-ikt},$$

$$u(x,t) = \hat{u}(x)e^{-ikt},$$

where k is the wave number then the system (2.7) reduces to

$$\Delta\hat{p} + k^2\hat{p} = 0. \tag{2.8}$$

The problem discussed here is to solve the system (2.7) for p and u subject to appropriate boundary conditions which will be discussed later.

The technique here is to drive the system (2.7) with a time harmonic source which will yield the time harmonic solutions, namely the solution of (2.8). This technique is essentially the numerical implementation of an appropriate limiting amplitude principle. For exterior problems this method has been demonstrated by Kriegsmann and Morawetz [6] and Taflove and Umashankar [12] and for wave guide problems by Baumeister [1] and Kriegsmann [7].

3. SOLUTION PROCEDURES

We take the origin at the open end of the duct so that its generators are parallel to the z axis (Figure 1). We look for solutions of (2.7) of the form

$$p(r,\theta,z,t) = P(r,z,t)e^{im\theta}$$
$$\underline{u}(r,\theta,z,t) = \underline{U}(r,z,t)e^{im\theta}. \tag{3.1}$$

In general solution will have the form

$$P = \sum_{m=0}^{\infty} P_m(r,z,t)e^{im\theta},$$

but we confine our solutions as in (3.1) for a single mode m. For $m \geq 1$ the solution is referred to as the spin mode solution. In physical situations they correspond to the modes provided by a turbofan engine. For $m = 0$ (3.1) describes a plane wave. The more important case is when $m > 0$ (a spinning mode). Then the system (2.7) becomes

$$\frac{\partial P}{\partial t} + u_z + v_r + \frac{v + imw}{r} = 0$$

$$\frac{\partial u}{\partial t} + \frac{\partial P}{\partial z} = 0$$

$$\frac{\partial v}{\partial t} + \frac{\partial P}{\partial r} = 0 \qquad (3.2)$$

$$\frac{\partial w}{\partial t} + \frac{im}{r} P = 0$$

and the problem reduces to solving the system (3.2) with appropriate boundary conditions.

The method we use to solve (3.2) is an explicit method which is fourth-order accurate in space and second-order accurate in time and is due to Gottlieb and Turkel [4]. This is a higher-order accurate version of the MacCormack scheme. The use of an explicit method has been recently advocated by Baumeister [1]. The major advantages are drastically reduced storage requirements and programming simplicity. Baumeister demonstrated the effectiveness of this approach for internal sound propagation with spinning modes [2]. The work in this paper extends this idea to the full radiation problem with a more accurate computational scheme.

A typical computational domain is depicted in Figure 2. Referring to this figure, the computations are carried out in the rectangular region which is bounded by an inflow boundary and the farfield boundary. Thickness of the duct is allowed by a mesh size thickness in the r direction. The solution for large times is extremely sensitive to the inflow condition and also the farfield condition [9]. The solution is assumed to start from a state of rest, i.e., $P = u = v = w = 0$ at time $t = 0$. The system (3.2) can be written in the form

$$\underline{w}_t + \underline{F}_z + \underline{G}_r = \underline{H} \ , \tag{3.3}$$

where

$$\underline{w} = \begin{bmatrix} P \\ u \\ v \\ w \end{bmatrix} , \quad \underline{F} = \begin{bmatrix} u \\ P \\ 0 \\ 0 \end{bmatrix} , \quad \underline{G} = \begin{bmatrix} v \\ 0 \\ P \\ 0 \end{bmatrix} , \quad \text{and} \quad \underline{H} = \begin{bmatrix} -\frac{v + imw}{r} \\ 0 \\ 0 \\ -\frac{imP}{r} \end{bmatrix} . \tag{3.4}$$

We use the method of time splitting to advance the solution from time t to $t + 2\Delta t$. If $L_z(\Delta t)$ and $L_r(\Delta t)$ denote symbolic solution operators to the one-dimensional equations

$$\begin{aligned} w^1_t + F_z &= H_1 \\ w^2_t + G_r &= H_2, \end{aligned} \tag{3.5}$$

then the solution to (3.3) is advanced by the formula

$$w(t + 2\Delta t) = L_z(\Delta t)\, L_r(\Delta t)\, L_r(\Delta t)\, L_z(\Delta t)\, w(t). \tag{3.6}$$

This procedure is second-order accurate in time. The fourth-order accuracy in space depends on formulating the difference scheme. For a one-dimensional system, i.e., for (3.5), we have

$$\begin{aligned} \overline{w}_i(t + \Delta t) &= w_i(t) + \frac{\Delta t}{6\Delta z}\left(7F_i - 8F_{i+1} + F_{i+2}\right) + \Delta t H_i \\ w_i(t + \Delta t) &= \frac{1}{2}\left[w_i(t) + \overline{w}_i(t + \Delta t) + \frac{\Delta t}{6\Delta z}\left(-7\overline{F}_i + 8\overline{F}_{i-1} - \overline{F}_{i-2}\right) + \Delta t\overline{H}_i\right], \end{aligned} \tag{3.7}$$

where $\overline{F}_i$ denote F evaluated at $\overline{w}_i$, etc. This formula contains a forward predictor and a backward corrector. This is second-order accurate in space. One can formulate another variant which contains a backward predictor and a forward corrector which is also second-order accurate in space. In order to achieve fourth-order accuracy we alternate (3.7) and its variant in each time step. If there are N intervals with nodes at $z_i(i=0,1,\cdots,N)$ then the predictor in (3.7) cannot be used at $i = N-1$ and at $i = N$ and the corrector cannot be used at $i = 0$ and 1. Similar situations occur for the other variant too. At these points we extrapolate the fluxes using third-order extrapolations. For the right boundary we use the extrapolation formulae

$$F_{N+1} = 4F_N - 6F_{N-1} + 4F_{N-2} - F_{N-3}$$

$$F_{N+2} = 4F_{N+1} - 6F_N + 4F_{N-1} - F_{N-2}, \tag{3.8}$$

and for the left boundary

$$F_0 = 4F_1 - 6F_2 + 4F_3 - F_4$$

$$F_1 = 4F_0 - 6F_1 + 4F_2 - F_3. \tag{3.9}$$

Since we are interested in time harmonic solutions, the numerical solution is monitored until the transient has passed out of the computational domain and the solution achieves a steady time harmonic dependence.

4. BOUNDARY CONDITIONS

A very important feature of our work is in obtaining appropriate boundary conditions. We derive our boundary conditions appropriate to an experiment carried out at NASA Langley Research Center [14]. The boundary conditions consists of two major parts. The first part is derivation of an inflow condition which will model correctly the sound source. Next, we need accurate farfield boundary conditions which will simulate outgoing radiation.

Inflow Conditions

To derive inflow boundary conditions we consider the time harmonic case and in particular equation (2.8). We look for spinning mode solutions of the form

$$\hat{p} = \bar{P}(r,z)e^{im\theta}.$$

This yields

$$\frac{1}{r}\frac{\partial}{\partial r}\left(r\frac{\partial \bar{P}}{\partial r}\right) + \left(k^2 - \frac{m^2}{r^2}\right)\bar{P} + \frac{\partial^2 \bar{P}}{\partial z^2} = 0. \tag{4.1}$$

If we separate variables by setting

$$\bar{P}(r,z) = f(r)\, g(z),$$

we obtain

$$f(r) = J_m(\beta r) \quad \text{and} \quad g(z) = e^{\pm i\ell z},$$

where

$$\beta^2 = k^2 - \ell^2, \tag{4.2}$$

and ℓ is to be determined.

If a is the radius of the duct (here $a = 1/2$ due to the non-dimensionalization) then the usual boundary condition on the pipe is the hard wall condition

$$\frac{\partial \hat{p}}{\partial n} = 0 \qquad \text{on} \quad r = a.$$

This gives

$$\frac{d}{dr}\left(J_m(\beta r)\right) = 0 \qquad \text{on} \quad r = a$$

or

$$\beta a = \lambda_{mn} \qquad (n=0,1,2,\cdots,)$$

where λ_{mn}'s are the zeros of the functions $J_m'(z)$. From (4.2), using the appropriate subscript corresponding to λ_{mn} we have

$$(\ell_{mn} a)^2 = (ka)^2 - \lambda_{mn}^2. \tag{4.3}$$

Definition: If $ka > \lambda_{mn}$, we say the mode (m,n) is cut-on. Otherwise it is said to be cut-off.

We now consider only cut-on modes. Then the solution of (4.1) has the form

$$\overline{P}(r,z) = \sum_{n=0}^{\infty} a_n e^{\pm iz\sqrt{(ka)^2 - \lambda_{mn}^2}} J_m\left(\frac{\lambda_{mn}}{a} r\right). \tag{4.4}$$

It is necessary to consider the case of a single cut-on mode propagating down the pipe. In this situation $n = 0$. Dropping the corresponding zero subscripts in (4.3) we consider the values of ℓ given by

$$\ell_m a = \sqrt{(ka)^2 - \lambda_m^2}\,.$$

Then the general solution inside the pipe can be written as a combination of an incoming wave and a reflected wave. That is

$$\hat{p}(r,\theta,z) = \left(e^{i\ell_m z} + R(k)e^{-i\ell_m z}\right) J_m\left(\lambda_m \frac{r}{a}\right)e^{im\theta}, \tag{4.5}$$

where R is the reflection coefficient and is also a function of the wave number k. Recalling that $p(r,\theta,z,t) = \hat{p}(r,\theta,z)e^{-ikt}$ and $p(r,\theta,z,t) = P(r,z,t)e^{im\theta}$ we have

$$P(r,z,t) = \left(e^{i\ell_m z} + R(k)e^{-i\ell_m z}\right) J_m\left(\lambda_m \frac{r}{a}\right)e^{-ikt}. \tag{4.6}$$

The reflection coefficient R is unknown. Thus we must eliminate R in (4.6). This is accomplished by taking the time derivative of (4.6) and subtracting the k/ℓ_m times the z derivative to get

$$P_t - \frac{k}{\ell_m} P_z = -2ik\, e^{i\ell_m z} J_m\left(\lambda_m \frac{r}{a}\right)e^{-ikt},$$

but

$$P_z = -u_t \qquad \text{from (3.2).}$$

Thus the above equation becomes

$$\left(P + \frac{k}{\ell_m} u\right)_t = -2ik\, e^{i\ell_m z} J_m\left(\lambda_m \frac{r}{a}\right) e^{-ikt}. \qquad \text{(I)}$$

We impose this boundary condition on the inflow boundary $z = -L$. We obtain boundary condition on v at the inflow by using (3.2),

$$\frac{\partial v}{\partial t} + \frac{\partial P}{\partial r} = 0,$$

together with

$$\frac{\partial P}{\partial r} = \frac{\lambda_m}{a} \frac{J_m'\left(\lambda_m \frac{r}{a}\right)}{J_m\left(\lambda_m \frac{r}{a}\right)} P$$

to give

$$\frac{\partial v}{\partial t} + \frac{\lambda_m}{a} \frac{J_m'\left(\lambda_m \frac{r}{a}\right)}{J_m\left(\lambda_m \frac{r}{a}\right)} P = 0. \qquad \text{(II)}$$

Note that the coefficient of P here contains a singular term at $r = 0$. However P contains a term (from (4.6)) of the form $J_m\left(\lambda_m \frac{r}{a}\right)$. Thus when $r = 0$ (II) is simply replaced by $v = 0$.

Conditions on the Wall

On the duct wall $\frac{\partial P}{\partial n} = \frac{\partial P}{\partial r} = 0$, but

$$\frac{\partial v}{\partial t} + \frac{\partial P}{\partial r} = 0 \qquad \text{from (3.2).} \qquad \text{(III)}$$

This implies $v = 0$ on the wall. We note that a general impedance condition simulating an acoustic liner can be handled without difficulty.

Conditions on the Axis

When $m = 0$ the system (3.2) has only three equations for p, u, and v. The first equation of (3.2) contains a $\frac{v}{r}$ term. Thus the boundary condition on the axis in this case is

$$v = 0 \qquad \text{on} \quad r = 0 \quad (m = 0). \tag{IV}$$

When $m = 1$ the last equation of (3.2) gives

$$\frac{\partial w}{\partial t} + \frac{im}{r} P = 0.$$

Here P contains a term like $J_1\left(\lambda \frac{r}{a}\right)$ for z close to $-L$. Thus $\frac{\partial w}{\partial t}$ is nonzero. But from the first equation of (3.2) we have

$$v + iw = 0 \qquad \text{on} \quad r = 0 \quad (m = 1). \tag{V}$$

For $m \geq 2$ the first and the last equations of (3.2) give

$$v = 0, \; w = 0 \qquad \text{on} \quad r = 0 \quad (m \geq 2). \tag{VI}$$

Farfield Conditions

Radiation conditions are applied at the farfield boundaries. The development follows that given in [3]. Let R be the distance $\left(R = \sqrt{r^2 + z^2}\right)$ from the origin to a point in the farfield (see Figure 2). The condition we impose here is the first member of a family of nonreflecting boundary conditions which are accurate as $R \to \infty$. This condition is

$$\frac{\partial P}{\partial t} + \frac{\partial P}{\partial R} + \frac{P}{R} = 0,$$

where

$$\frac{\partial P}{\partial R} = \frac{\partial P}{\partial z} \cos \alpha + \frac{\partial P}{\partial r} \sin \alpha,$$

where α is the angle from the z axis to the farfield point. Using the second and third equations of (3.2) we have

$$\frac{\partial P}{\partial R} = - u_t \cos \alpha - v_t \sin \alpha.$$

Thus the radiation condition becomes

$$\frac{\partial P}{\partial t} - (u \cos \alpha + v \sin \alpha)_t + \frac{P}{R} = 0. \qquad \text{(VII)}$$

The conditions I through VII were used to obtain the results discussed in the next section.

5. NUMERICAL RESULTS

We computed the solutions with the details given in Sections 3 and 4 on a CDC Corp. Cyber-203 machine. The algorithm described above is almost totally vectorizable. For a very low frequency plane wave case the typical number of grid points in the r,z plane were 80×100. The inflow boundary was kept at $z = -10d$ (10 diameters) and the radiation boundary was chosen so as to enclose a circle of radius $10d$. For high frequencies the typical grid sizes were 115×135 and the inflow boundary as varied from $z = -10d$ to $z = -8d$.

To verify the effectiveness of the code we compared our results with asymptotic expansion obtained by Ting and Keller [13] for a low frequency

plane wave. To make comparisons we computed the solutions in the duct and on the axis at various stations for a non-dimensional frequency $ka = 0.2$. Here $k = \frac{2\pi}{\omega}$ is the wave number. Results are presented in Table I.

For high frequencies we compared our results with the Weiner-Hopf results of Savkar and Edelfelt [11] and the experiment done at NASA Langley Research Center [14]. In this experiment the directivity patterns were measured on a circle at 10 diameters from the open end of the pipe. The test facility has a spin mode synthesizer which can produce both plane and spinning mode wave.

The first comparison was made for the plane wave case $(m = 0)$ and a non-dimensional frequency of $ka = 3.76$. Since the experimental results were obtained only in the farfield the sound pressure level was plotted as a function of angle measured from z axis. The results are presented in Figure 3 and show good agreement with the experiment.

Figures 4 and 5 show typical comparisons of the spinning mode case with $m = 2$ and for frequency values $ka = 3.37$ and 4.40. As in these figures, except the plane wave case, the computed results agree within 5 dB levels. Clearly our results show better comparison than Weiner-Hopf results [11] due to allowance of thickness. In these cases the results near the axis do not compare very well. This is due to the fact that in the experiment it is difficult to completely control other modes and plane waves. This is particularly true for this frequency $ka = 4.40$ which is close to the next cut-on mode. In the plane wave case the results were unexpectedly good.

6. VARIABLE GEOMETRY DUCTS

We consider ducts with a local variable geometry cross section. The duct is assumed to be straight as $z \to -\infty$ (see Figure 4). Thus the inflow boundary conditions previously formulated are still valid. The variable duct is incorporated in the numerical scheme by mapping it into a straight duct. This slightly changes the coefficients in the final system (3.3) but does not degrade the convergence to the time harmonic solution.

Suppose the duct configuration is as in Figure 4. It has a curved boundary near $z = 0$ and has straight extension everywhere else. This allows us to have the same inflow boundary conditions and the conditions on axis and also the radiation condition. But the boundary conditions on the wall will be changed.

The Euler equations have the form

$$w_t + f_z + g_r + h = 0. \tag{6.1}$$

We do the following maps:

$$\begin{aligned} z_1 &= z \\ r_1 &= \frac{r}{an(z)} . \end{aligned} \tag{6.2}$$

We use chain rule to compute f_z, g_r in terms of f_{z_1} and g_{r_1}, etc. where $r = n(z)$ is the geometry of the duct. This yields

$$w_t + f_{z_1} + \left(\frac{1}{an(z)}\, g - \frac{rn'(z)}{an(z)^2}\, f\right)_{r_1} + f\,\frac{n'(z)}{n(z)} + h = 0. \tag{6.3}$$

This has the same form as (6.1). Thus very minor changes in the difference scheme and in the radiation boundary conditions are required. The boundary condition $v = 0$ on $r = a$ is replaced by the vanishing of the normal velocity on the wall. On the surface of the pipe a normal vector is $(1, -an'(z))$ in (r,z) coordinates. Thus the above condition reduces to

$$v - an'(z)u = 0. \tag{6.4}$$

We simulated a duct where $n(z)$ has the form

$$n(z) = \begin{cases} .5 & z < -1 \\ .5 - \varepsilon(2z-1)(z+1)^2 & -1 \leq z \leq 0 \end{cases},$$

(see Figure 4). The grids of the computational domain follow the same geometry. For $\varepsilon = .15$ the results we obtained are shown in Figure 6 compared with the straight duct situation. The dB level reduces at 90^o by about 10 dB. This indicates the importance of the nozzle geometry in determining the farfield radiation pattern.

REFERENCES

[1] K. J. BAUMEISTER, Numerical Techniques in Linear Duct Acoustics, NASA TM-82730, 1981.

[2] K. J. BAUMEISTER, Influence of exit impedance on finite difference solutions of transient acoustic mode propagation in ducts, ASME Paper No. 81-WA/NCA-13, 1981.

[3] A. BAYLISS and E. TURKEL, Radiation boundary conditions for wave-like equations, Comm. Pure Appl. Math., 33, No. 6 (1980), pp. 707-725.

[4] D. GOTTLIEB and E. TURKEL, Dissipative two-four methods for time dependent problems, Math. Comp., 30 (1976), pp. 703-723.

[5] S. J. HOROWITZ, R. K. SIGMANN and B. T. ZINN, Iterative finite element - integral technique for predicting sound radiation from turbofan inlets, AIAA Paper 81-1981, 1981.

[6] G. A. KRIEGSMANN and C. S. MORAWETZ, Solving the Helmholtz equation for exterior problems with a variable index of refraction, SIAM J. Sci. Statis. Comput., 1 (1980), pp. 371-385.

[7] G. A. KRIESGMANN, Radiation conditions for wave guide problems, SIAM J. Sci. Statis. Comput., 3 (1982), pp. 318-326.

[8] H. LEVINE and J. SCHWINGER, On the radiation of sound from an unflanged circular pipe, Phys. Rev., 73 (1948), pp. 383-406.

[9] L. MAESTRELLO, A. BAYLISS and E. TURKEL, On the interaction between a sound pulse with shear layer of an axisymmetric jet, J. Sound Vib., 74 (1981), pp. 281-301.

[10] S. D. SAVKAR, Radiation of cylindrical duct acoustics modes with flow mismatch, J. Sound Vib., 42 (1975), pp. 363-386.

[11] S. D. SAVKAR and I. H. EDELFELT, Radiation of Cylindrical Duct Acoustic Modes with Flow Mismatch, NASA CR-132613, 1975.

[12] A. TAFLOVE and K. R. UMASHANKAR, Solution of Complex Electromagnetic Penetration and Scattering Problems in Unbounded Regions, Computational Methods for Infinite Domain Media-Structure Interaction, A. J. Dalinowski, ed., (1981), pp. 83-114.

[13] L. TING and J. B. KELLER, Radiation from the open end of a cylindrical or conical pipe and scattering from the end of a rod or slab, J. Acoust. Soc. Amer., 61 (1977), pp. 1439-1444.

[14] J. M. VILLE and R. J. SILCOX, Experimental Investigation of the Radiation of Sound from an Unflanged Duct and a Bellmouth Including the Flow Effect, NASA TP-1697, 1980.

Table I. Comparison with Ting and Keller Solution
ka = 0.2

Z	Ting & Keller |P|	Numerical |P|
-10	1.5026	1.5054
- 9	1.0984	1.1113
- 8	.3873	.3544
- 7	.4355	.3933
- 6	1.1133	1.0874
- 5	1.7603	1.7196
- 4	1.9280	1.9583
- 3	1.8933	1.9097
- 2	1.5495	1.5477
- 1	1.0279	1.0076

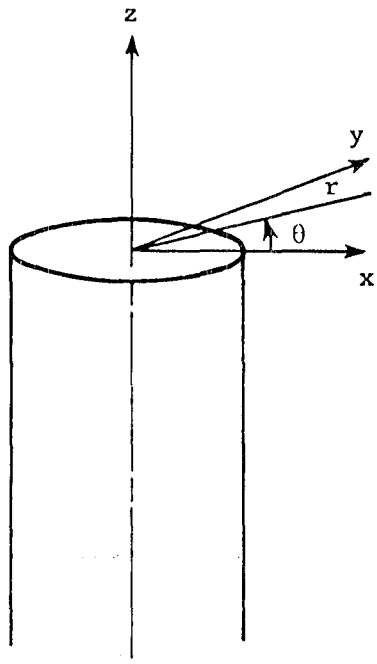

Figure 1.

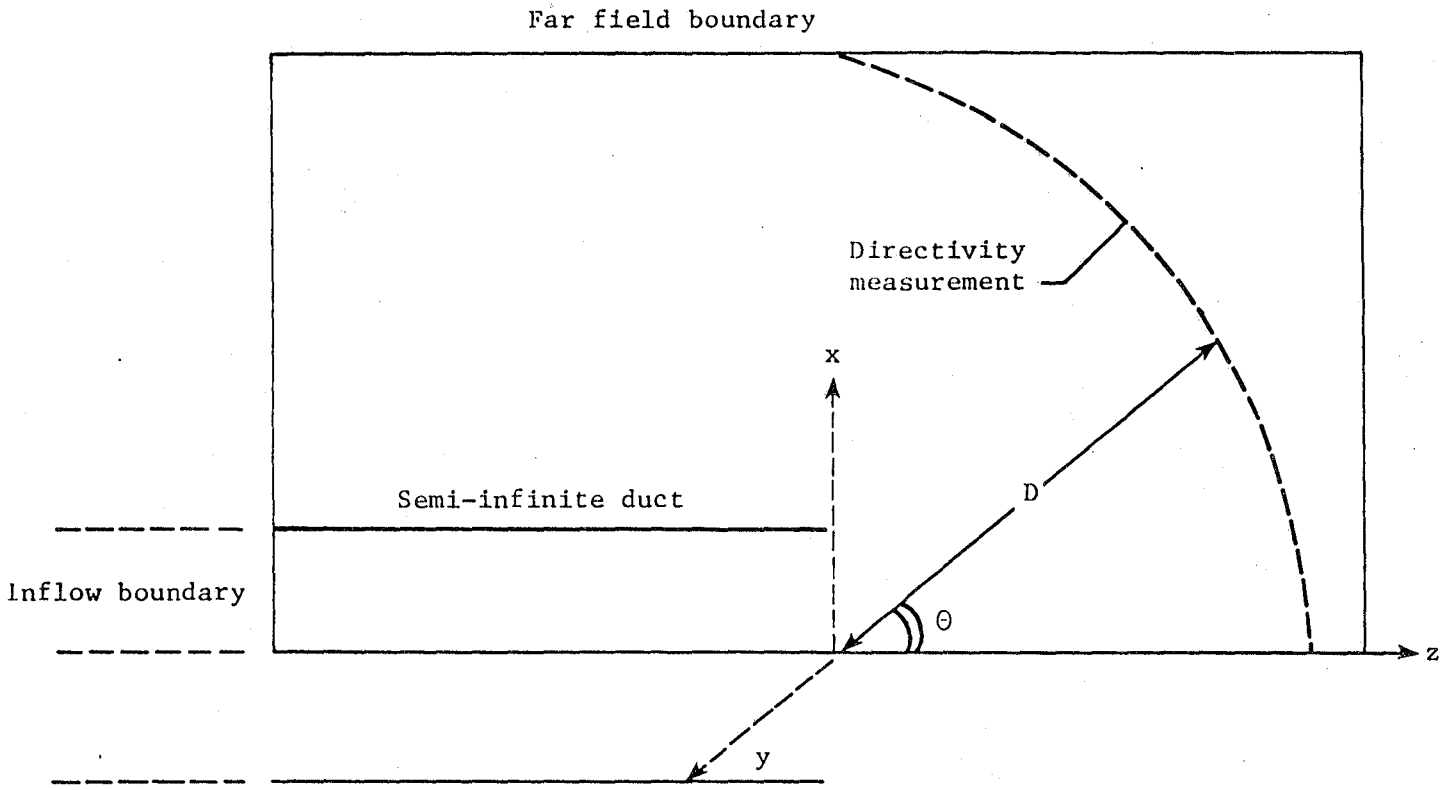
Far field boundary
Directivity
measurement
x
Semi-infinite duct
D
Inflow boundary
Θ
z
y

Figure 2.

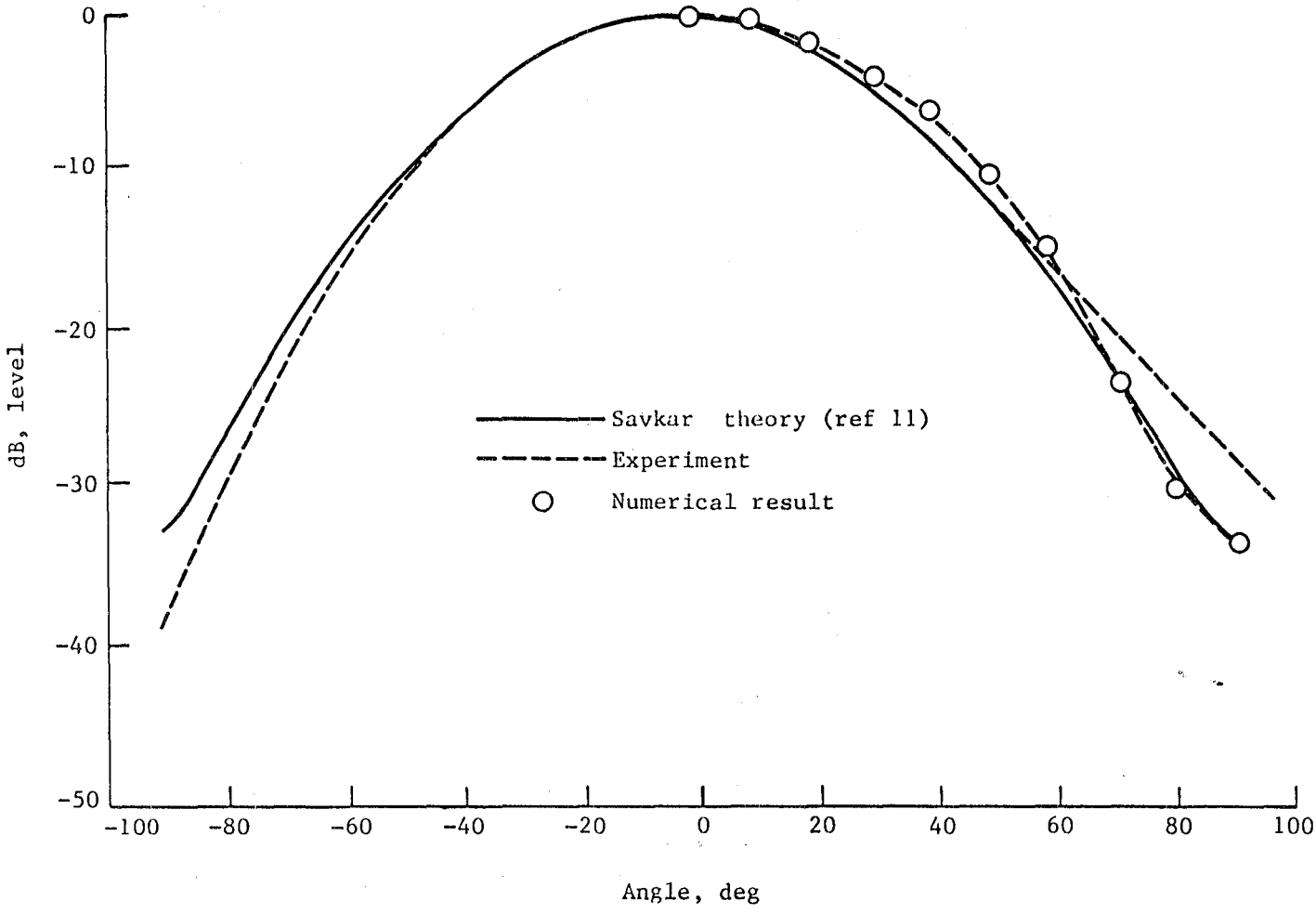
0
-10
-20
-30
-40
-50
dB, level
-100
-80
-60
-40
-20
0
20
40
60
80
100
Angle, deg
Savkar theory (ref 11)
Experiment
Numerical result

Figure 3.

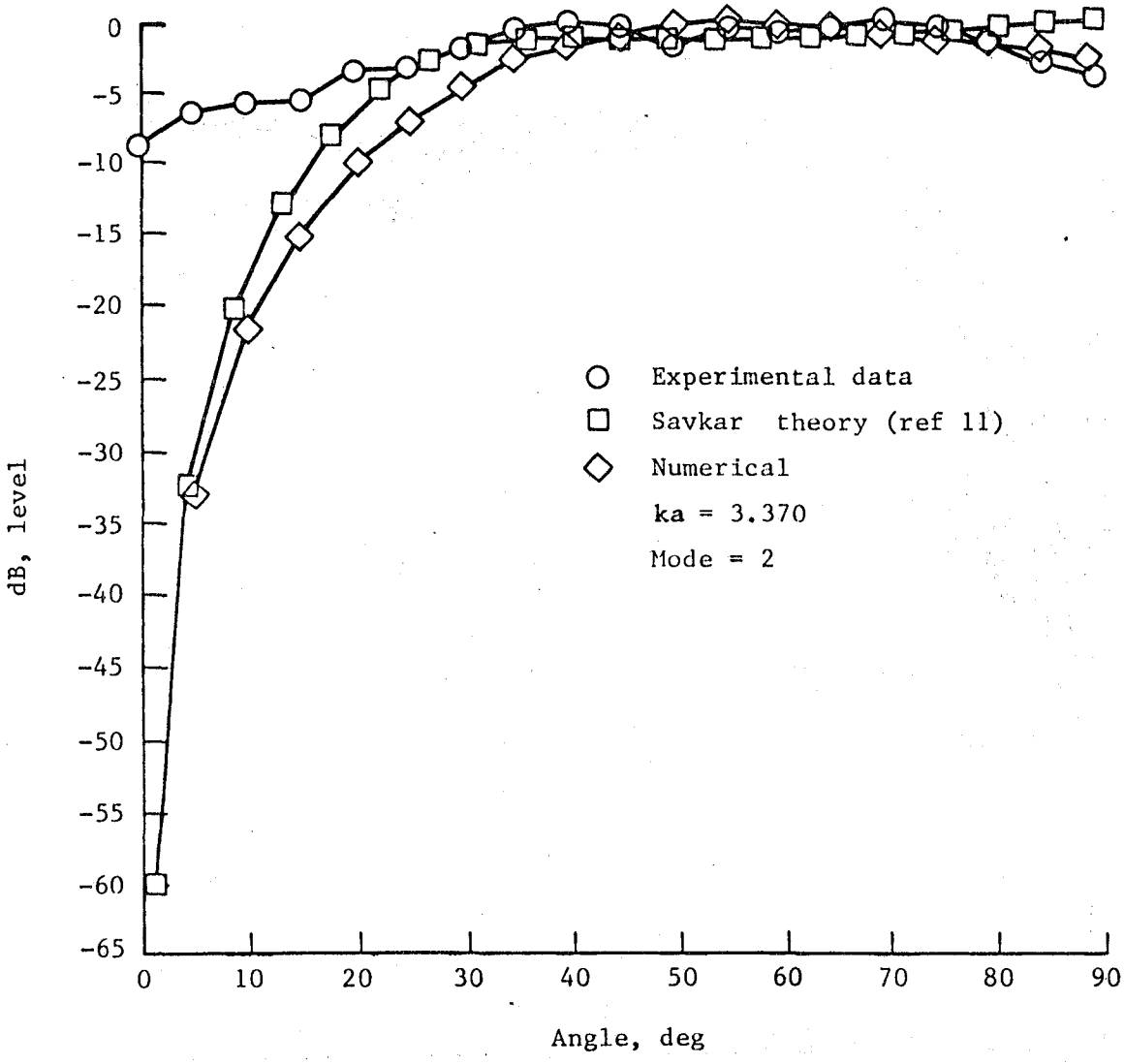
0
-5
-10
-15
-20
-25
-30
-35
-40
-45
-50
-55
-60
-65
dB, level
0
10
20
30
40
50
60
70
80
90
Angle, deg
Experimental data
Savkar theory (ref 11)
Numerical
ka = 3.370
Mode = 2

Figure 4.

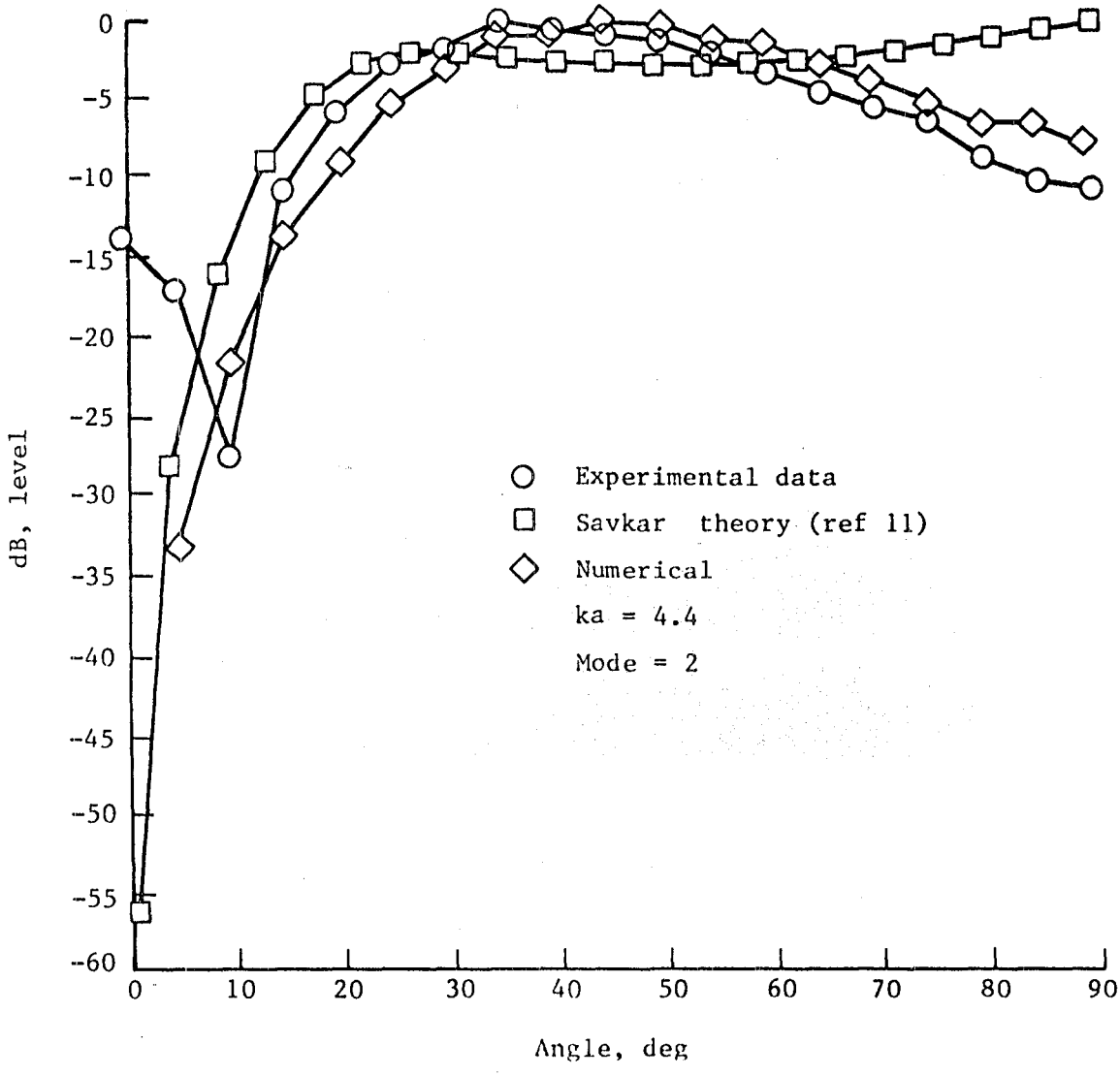
0
-5
-10
-15
-20
-25
-30
-35
-40
-45
-50
-55
-60
dB, level
0
10
20
30
40
50
60
70
80
90
Angle, deg
Experimental data
Savkar theory (ref 11)
Numerical
ka = 4.4
Mode = 2

Figure 5.

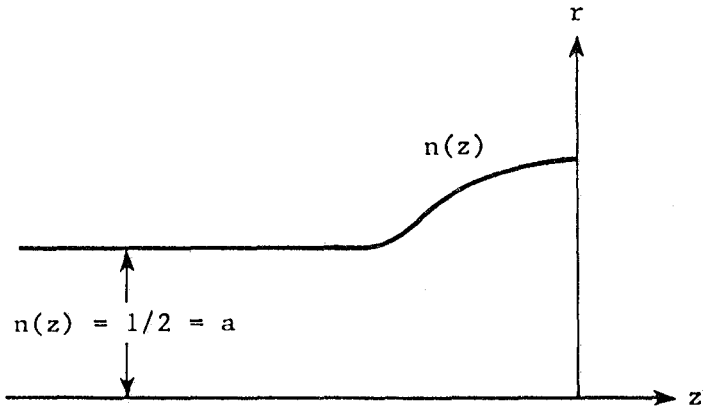

Figure 6.

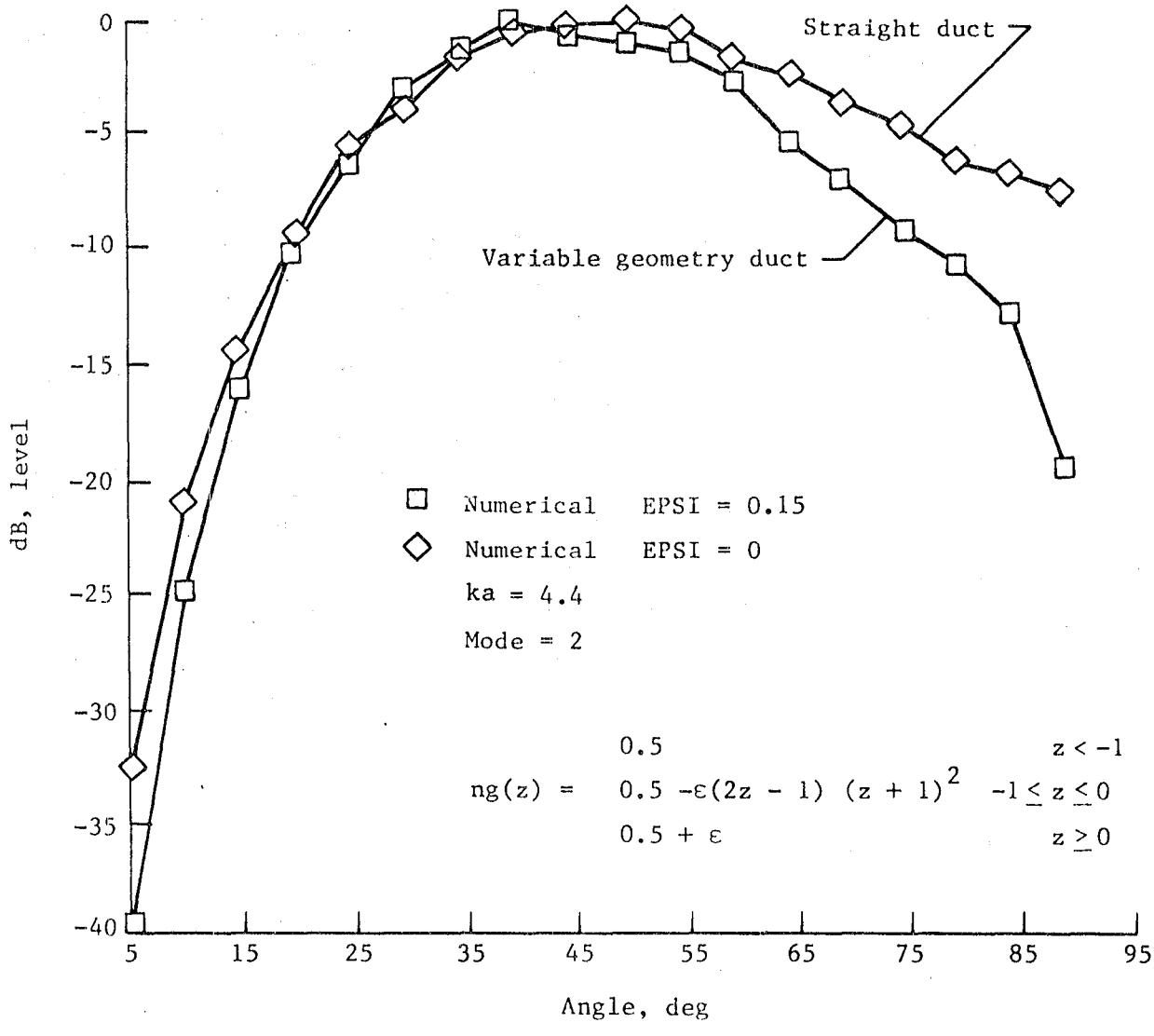
Straight duct
Variable geometry duct
Numerical EPSI = 0.15
Numerical EPSI = 0
ka = 4.4
Mode = 2
ng(z) = 0.5 z < -1
0.5 -ε(2z - 1) (z + 1)^2 -1 ≤ z ≤ 0
0.5 + ε z ≥ 0
dB, level
0
-5
-10
-15
-20
-25
-30
-35
-40
5
15
25
35
45
55
65
75
85
95
Angle, deg

Figure 7.

1. Report No.	2. Government Accession No.	3. Recipient's Catalog No.
NASA CR-172171		

4. Title and Subtitle	5. Report Date
Radiation of Sound from Unflanged Cylindrical Ducts	July 1983
	6. Performing Organization Code

7. Author(s)	8. Performing Organization Report No.
S. I. Hariharan and A. Bayliss	83-32
	10. Work Unit No.

9. Performing Organization Name and Address	11. Contract or Grant No.
Institute for Computer Applications in Science and Engineering Mail Stop 132C, NASA Langley Research Center Hampton, VA 23665	NAS1-17070
	13. Type of Report and Period Covered
12. Sponsoring Agency Name and Address National Aeronautics and Space Administration Washington, D.C. 20546	Contractor report
	14. Sponsoring Agency Code

15. Supplementary Notes
Additional support: U. S. Department of Energy, Contract No. TE/AC02/76ER03077, Air Force Contract No. AFOSR/81/0020.
Langley Technical Monitor: Robert H. Tolson
Final Report

16. Abstract

In this paper we present calculations of sound radiated from unflanged cylindrical ducts. The numerical simulation models the problem of an aero-engine inlet. The time-dependent linearized Euler equations are solved from a state of rest until a time harmonic solution is attained. A fourth-order finite difference scheme is used. Solutions are obtained from a fully vectorized Cyber-203 computer program. Cases of both plane waves and spin modes are treated. Spin modes model the sound generated by a turbofan engine. Boundary conditions for both plane waves and spin modes are treated. Solutions obtained are compared with experiments conducted at NASA Langley Research Center.

17. Key Words (Suggested by Author(s))	18. Distribution Statement
duct acoustics sound radiation radiation pattern finite differences	64 Numerical Analysis Unclassified-Unlimited

19. Security Classif. (of this report)	20. Security Classif. (of this page)	21. No. of Pages	22. Price
Unclassified	Unclassified	29	A03

End of Document